JACC: CARDIOVASCULAR INTERVENTIONS VOL. 6, NO. 8, 2013

ISSN 1936-8798/$36.00
PUBLISHED BY ELSEVIER INC. http://dx.doi.org/10.1016/j.jcin.2013.03.019

Incidence, Predictors, Morphological Characteristics, and Clinical Outcomes of Stent Edge Dissections Detected by Optical Coherence Tomography

Daniel Chamié, MD, Hiram G. Bezerra, MD, PhD, Guilherme F. Attizzani, MD, Hirosada Yamamoto, MD, Tomoaki Kanaya, MD, Gregory T. Stefano, MD, Yusuke Fujino, MD, Emile Mehanna, MD, Wei Wang, PhD, Ahmad Abdul-Aziz, BS, Matthew Dias, BS, Daniel I. Simon, MD, Marco A. Costa, MD, PhD

Cleveland, Ohio

Objectives This study sought to investigate the frequency, predictors, and detailed qualitative and quantitative assessment of optical coherence tomography (OCT)-detected stent edge dissections. Its impact on subsequent management and clinical outcomes were also investigated.

Background OCT is a high-resolution imaging modality that can lead to more frequent recognition and accurate assessment of vascular injuries during percutaneous coronary intervention (PCI).

Methods From September 2010 to June 2011, all patients with OCT post-PCI were enrolled. Edge dissections were defined as disruptions of the arterial lumen surface in both the 5-mm distal and proximal stent edges. Qualitative and quantitative analyses of all edges were performed at 0.2-mm intervals.

Results In total, 395 edges (249 lesions in 230 patients) were analyzed. The overall incidence of OCT-detected edge dissection was 37.8%, and most (84%) were not apparent on angiography. Independent predictors for OCT-detected dissections were presence of atherosclerotic plaque at stent edges, calcification angle, minimum fibrous cap thickness, thin-cap fibroatheromas, stent/lumen eccentricity, and vessel overstretching. Mean dissection length measured 2.04 $\pm$ 1.60 mm, 96.2% appeared as flaps, and 52.8% extended beyond the intima/atheroma layer. Additional stenting was performed in 22.6% of all dissections, which were longer, had bigger dimensions, and promoted deeper vascular injury. The 12-month major adverse cardiac event rate was similar between patients with (7.95%) and without (5.69%, $p = 0.581$) dissections.

Conclusions High rates of stent edge dissections were detected by OCT, usually related to the presence of atherosclerosis at stent edges and to PCI technique. Detailed OCT assessment of dissection severity was possible and affected the subsequent management of this complication. Non–flow-limiting, small, and superficial dissections left untreated proved benign. (J Am Coll Cardiol Intv 2013;6:800–13) © 2013 by the American College of Cardiology Foundation

From the Division of Cardiology, Harrington Heart & Vascular Institute, University Hospitals Case Medical Center, Case Western Reserve School of Medicine, Cleveland, Ohio. Dr. Bezerra has received honoraria and research funding from St. Jude Medical. Dr. Attizzani has received consultant fees from St. Jude Medical. Dr. Stefano has served as a consultant for St. Jude Medical. Dr. Simon has served on the advisory boards of Medtronic Vascular, Cordis/Johnson & Johnson, Merck, and Janssen/Johnson & Johnson. Dr. Costa has received honoraria and research funding from St. Jude Medical, and is on their Speakers' Bureau. All other authors have reported that they have no relationships relevant to the contents of this paper to disclose.

Manuscript received January 16, 2013; revised manuscript received March 18, 2013, accepted March 22, 2013.

Plaque fracture and dissection of the arterial wall are key mechanisms of lumen enlargement after balloon angioplasty (1,2). During stent implantation, unplanned vessel tearing may occur at the transition between the rigid stent struts and the adjacent arterial wall (3), which has been associated with increased risks of thrombosis and major adverse cardiac events (MACE) (4–8).

Coronary angiography (9) and intravascular ultrasound (IVUS) (3,10) have traditionally been used for the diagnosis of dissections at stent edges. Reported incidences of stent edge dissection range from 5% to 23% of the percutaneous coronary intervention (PCI) procedures as detected by IVUS (3). The superior resolution (12 to 18 μm) (11) of light-based optical coherence tomography (OCT) compared with IVUS (150 to 250 μm) may lead to more frequent recognition of vascular injury during PCI (12,13). Although physicians welcome better imaging and more knowledge of the vascular response to PCI, they face a clinical dilemma on the subsequent management of OCT findings. Recent reports provided early insights on the incidence and characteristics of stent edge dissections by OCT (14,15), but the inherent selection bias of retrospective, small studies have limited our understanding of the true incidence and clinical implications of OCT-detected stent edge dissections. Therefore, the goals of the present study were to: 1) determine the frequency of stent edge dissections by OCT in a large, unrestricted population representative of the daily clinical practice; 2) perform a detailed morphometric assessment of stent edge dissections and identify potential factors associated with its occurrence; 3) assess the impact of the OCT findings on the clinical management of edge dissections in real practice; and 4) examine the clinical outcomes of OCT-detected edge dissections.

Methods

Study population, study design, and PCI procedures. OCT was adopted as the standard intravascular imaging modality at our Institution after its approval by the U.S. Food and Drug Administration in May 2010. The University Hospitals Case Medical Center OCT Program is a prospective initiative approved by the local institutional review board, and comprises 2 distinct phases: Phase I (September to October 2010) was a quality initiative program designed to evaluate safety, feasibility, and clinical impact of OCT usage on patient management in the daily practice. During this phase, OCT was performed in all patients undergoing a coronary intervention or requiring an invasive evaluation of intermediate coronary lesions (16). There were no pre-defined exclusion criteria, thus representing an "all-comers," unrestricted use of OCT; Phase II, from November 2010 onward, comprised the "real-world" clinical utilization of OCT per the operator's discretion, thus representing a "selective use" of OCT in routine practice. All patients submitted to OCT examination from September 2010 to June 2011 were prospectively entered into a dedicated database, and comprise the population included in the current analysis.

PCI was performed per standard practice. Patients were treated with a loading dose of aspirin 300 mg and clopidogrel 300 mg or 600 mg. At the beginning of the procedure, a weight-adjusted (100 IU/kg) bolus of unfractionated heparin or a bolus of bivalirudin (0.75 mg/kg) was administered. Additional heparin boluses or continuous intravenous infusion of bivalirudin 1.75 mg/kg/h were given in order to maintain an activated clotting time ≥250 s. Glycoprotein IIb/IIIa inhibitors were used as per the operator's discretion. OCT imaging was mandatory in Phase I and left at the operator's discretion during Phase II. No formal recommendations were given regarding the management of stent edge dissection identified by OCT, which allowed proper assessment of the operator reaction to OCT findings without bias.

Angiographic analysis. All angiograms were analyzed off-line for the presence of stent edge dissections by 2 experienced interventional cardiologists blinded to the OCT findings. The target lesion was classified according to the American College of Cardiology/American Heart Association classification system (17). Severe calcification was characterized by the presence of radiopacities noted without cardiac motion before contrast injection, and generally compromising both sides of the arterial lumen (18). Severe angulation was defined as an artery bend >60° (17). Haziness was characterized as the presence of nonhomogeneous reduced contrast density within the arterial lumen, not fulfilling the criteria of definite thrombus or dissection (19,20). The step-up/step-down phenomenon was characterized by an abrupt transition of the vessel caliber between the proximal and distal stent borders to its respective references (21). Severity of stent edge dissections was classified according to the National Heart, Lung, and Blood Institute criteria as types A through F (9). Final coronary epicardial flow was classified according to the Thrombolysis In Myocardial Infarction criteria from 0 to 3 (22).

Abbreviations and Acronyms

FC = fibrous cap
IVUS = intravascular ultrasound
MACE = major adverse cardiac event(s)
MI = myocardial infarction
OCT = optical coherence tomography
OR = odds ratio
PCI = percutaneous coronary intervention
TCFA = thin-cap fibroatheroma

OCT image acquisition and analysis. OCT images were acquired with a commercially available Fourier-Domain OCT system (C7 XR OCT Intravascular Imaging System, St. Jude Medical, St. Paul, Minnesota) after intracoronary administration of 100 to 200 μg of nitroglycerin (unless clinically contraindicated) through conventional 6-F or 7-F guiding catheters. A 0.014-inch angioplasty guidewire was

positioned distally in the target vessel, and the OCT catheter (C7 Dragonfly, St. Jude Medical) was advanced at least 10 mm distal to the distal stent edge. The entire length of the stented region was scanned using an integrated automated motorized pullback device at a speed of 20 mm/s. Continuous flush of iodine contrast medium (8 to 20 ml), through a power injector (3 to 7 ml/s at 300 psi), was performed to create a virtually blood-free environment and to trigger image acquisition. In cases with stented segments longer than 54 mm (the maximum scan length of the current OCT system), performance of another pullback was recommended to ensure visualization of the proximal stent edge. All OCT images were digitally stored and submitted to the institution's cardiovascular imaging core laboratory for off-line independent analysis.

All OCT runs were carefully screened for quality, and stent edges with <5 mm length or those with poor visualization due to artifacts or inadequate blood clearance were

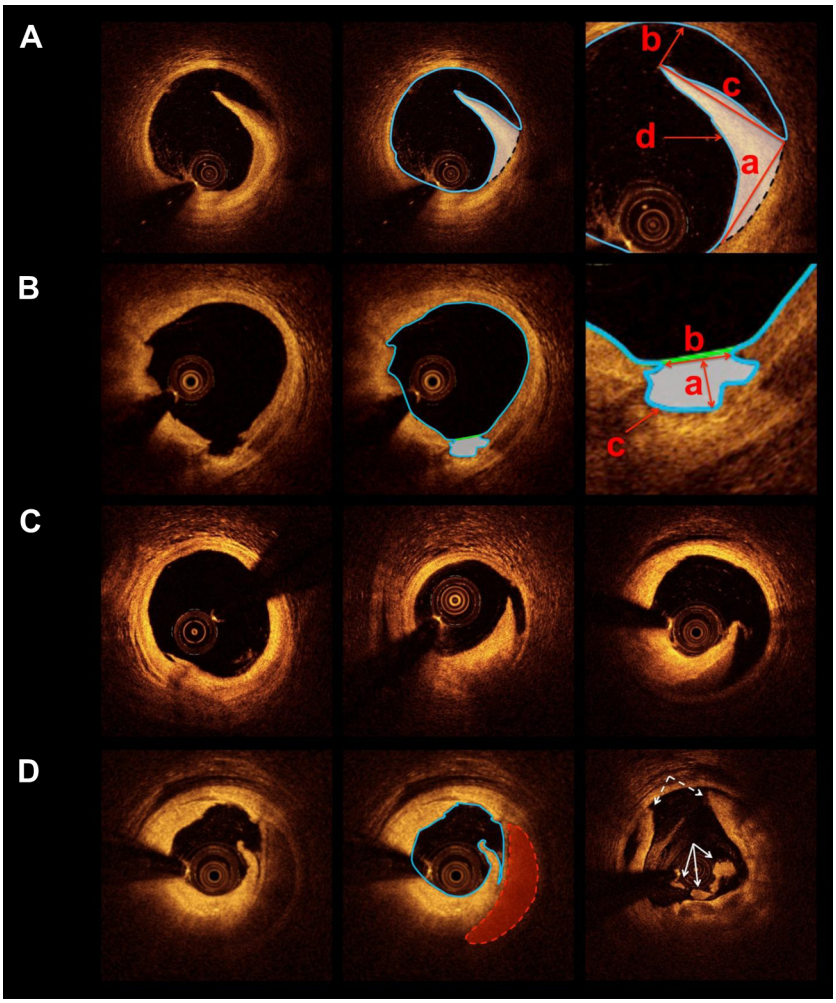

Figure 1. OCT Qualitative and Morphometric Assessment of Stent Edges

(A) Left: dissection flap; **center**: lumen segmentation outlining the flap **(solid blue tracing)**; **right**: flap morphometric parameters: **a**. depth—distance from the luminal surface to the joint point with the vessel wall at the base of the flap; **b**. opening—distance from the tip of the flap to the lumen contour along a line projected through the gravitational center of the lumen; **c**. length—measured from the tip of the flap to the joint point of the flap with the vessel wall; and **d**. area **(white region)**—planimetry of the region outlined by the lumen contours incorporating **(solid blue tracing)** and interpolating **(black dotted tracing)** the flap. **(B) Left**: dissection cavity; **center**: lumen segmentation outlining the cavity region **(solid blue tracing)** and another contour overlapping the first and interpolating each side of the cavity **(solid green tracing)**; **right**: cavity morphometric parameters: **a**. depth–line projected through the gravitational center of the lumen from the deepest point inside the cavity to the second lumen contour; **b**. opening—distance between the points where the 2 lumen contours intersect; and **c**. area **(white region)**—planimetry of the lumen area bounded by the 2 lumen contours. **(C)** Dissection axial depth—**left**: intimal; **center**: medial; **right**: adventitial. **(D) Left**: flap dissection with intramural hematoma; **center**: lumen **(blue contour)** and hematoma area segmentation **(red shaded region)**; and **right**: dissection flap **(dotted white arrow)** with intraluminal white thrombus **(solid white arrow)**. OCT = optical coherence tomography.

excluded. All images were analyzed at 0.2-mm (every-frame) intervals with dedicated automated contour-detection software (OCT system software B.0.1, St. Jude Medical).

Stent borders were defined as the first and last cross sections of the stented segment where struts could be seen in all 4 quadrants of the image. The peristent region consisted of the first frame immediately following the stent border (0.2 mm apart). Stent edges were defined as the 5-mm regions immediately adjacent to the stent borders, both distally and proximally. Edge dissection was defined as disruptions of the arterial lumen surface in the stent edge segment seen in at least 2 consecutive cross-section images. Its longitudinal length was calculated by multiplying the number of consecutive cross sections containing dissection by the slice thickness (pullback speed [mm/s] × frame rate [s]).

Dissections were morphologically classified as flaps and cavities. Specific morphometric parameters for each flap (Fig. 1A) and cavity (Fig. 1B) were calculated to estimate the magnitude of dissections.

The severity of each dissection was further estimated according to a qualitative assessment of the depth of vessel injury as: 1) intimal (limited to the intima layer or atheroma); 2) medial (extending into the media layer); and 3) adventitial (extending through the external elastic membrane) (23) (Fig. 1C). Presence of intramural hematoma was defined as an accumulation of flushing medium (or blood) within the

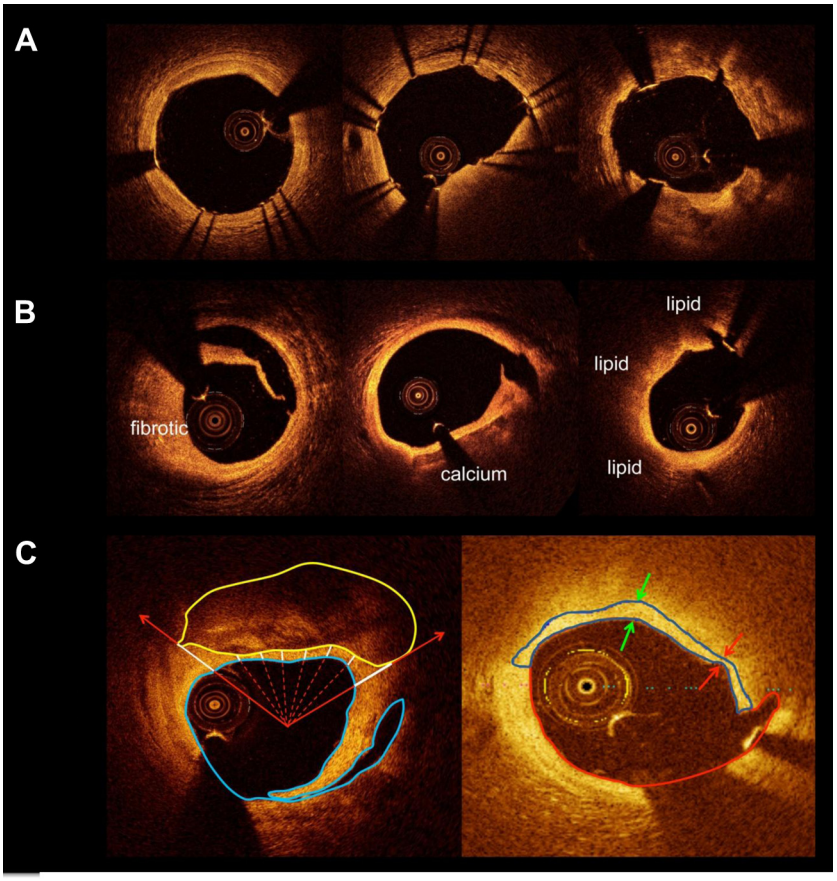

Figure 2. Relationship of Atherosclerotic Disease at Stent Edges and Dissections

(A) Stent landing zone assessment—stent borders were positioned over a "normal" vessel segment **(left)** or a diseased region with eccentric **(center)** or circumferential **(right)** plaque distribution. **(B) Left**: fibrotic plaque–related dissection; **center**: fibrocalcified plaque–related dissection; **right**: lipid-rich plaque–related dissection. **(C) Left**: calcification **(solid yellow contour)** quantification. Circumferential calcium distribution (degrees of arc) was measured using a protractor centered on the lumen **(red solid arrows)**. Calcium-to-lumen distance **(white solid lines)** was determined as the distance between the luminal edge of the calcium and the lumen contour at a 15° interval **(red dotted lines)**, and the average value was taken; **right**: fibrous cap (FC) quantification in lipid-rich plaques. The luminal boundary of the FC coincides with the lumen contour, and the abluminal boundary was automatically identified by a dynamic program algorithm that discriminates the optimal pixel intensity transition between the FC and lipid/necrotic core. The minimal distance from every locus in the luminal boundary of the FC to its abluminal boundary was automatically computed, and the minimum and mean FC thicknesses were recorded. FC surface area was determined as the product of the frame interval, and the arc length of the FC summed over involved frames (26). The red and green arrows indicate the minimum and maximum FC thicknesses, respectively.

medial space, displacing the internal elastic membrane inward and the external elastic membrane outward (23). The intramural hematoma area was determined by planimetry, and its longitudinal length calculated (Fig. 1D). Intraluminal thrombus was characterized as a mass attached to the luminal surface or floating within the lumen (23) (Fig. 1D).

Presence of atherosclerotic disease at the stent edges was investigated (Fig. 2). A "normal" vessel was characterized by the presence of a 3-layered architecture comprising the evidence of intimal, medial, and adventitial layers (23) with an intimal thickness <250 μm (24). Whenever atherosclerotic disease was present, plaques were classified according to previously described criteria as fibrotic, fibrocalcific, or lipid-rich (23,25) (Fig. 2B). Circumferential distribution of calcium and calcium-to-lumen distance were determined for all calcified plaques (Fig. 2C). In lipid-rich plaques, the entire extension of the overlying fibrous cap (FC) was semiautomatically segmented using a custom-built software, and the FC surface area and its minimum and mean thicknesses were automatically calculated (26) (Fig. 2C). Thin-cap fibroatheroma (TCFA) was defined as a lipid-rich plaque with minimum FC thickness ≤65 μm (27).

At the stent border, the stent area was measured, and the stent eccentricity index was calculated as: (maximum stent diameter − minimum stent diameter)/maximum stent diameter. Lumen eccentricity index was determined as (maximum lumen diameter − minimum lumen diameter)/maximum lumen diameter. Lumen area stenosis was calculated as: ([mean lumen area − minimum lumen area]/mean lumen area × 100). Stent diameter/lumen diameter ratio

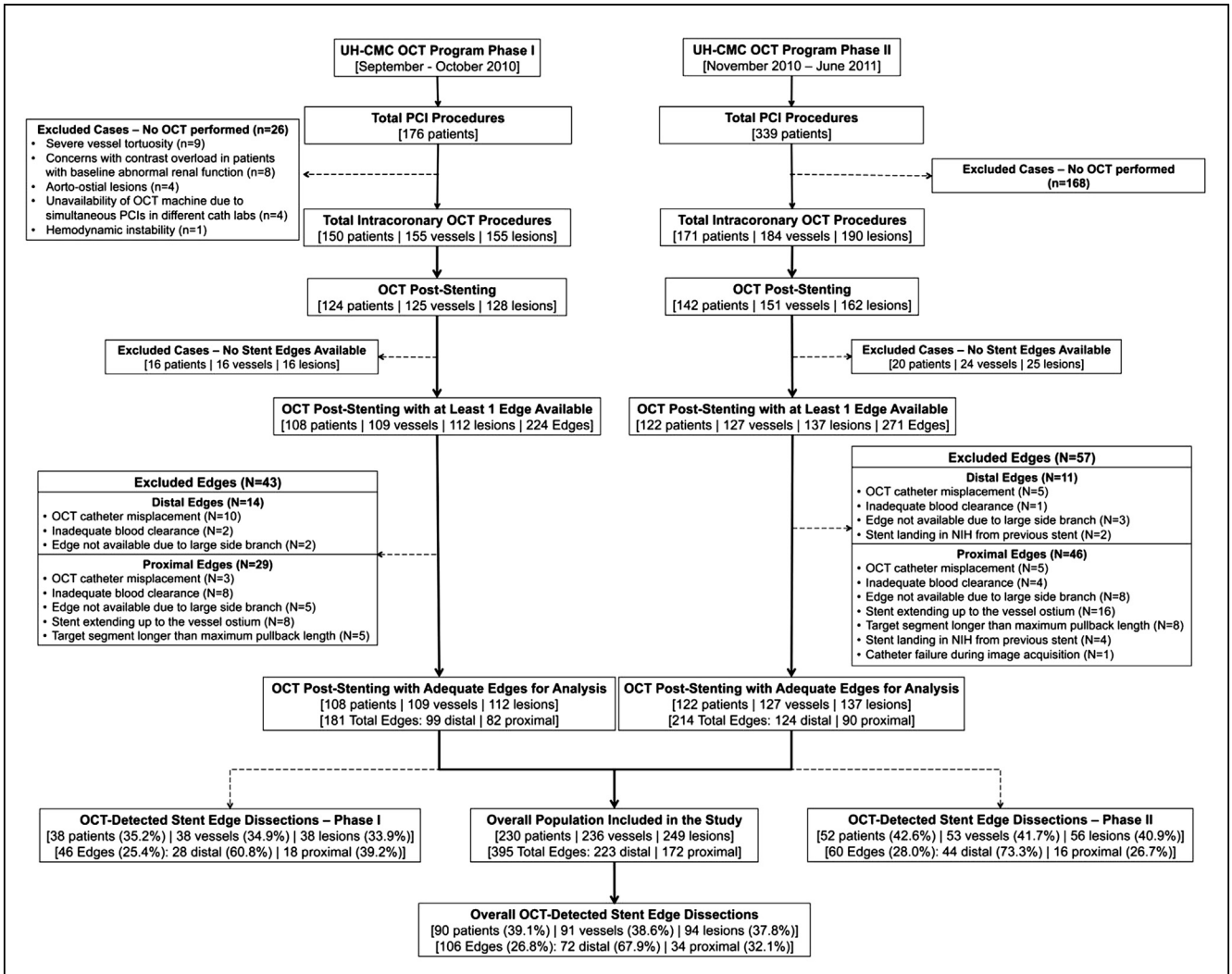

Figure 3. Study Flowchart

Flowchart showing inclusion and exclusion of subjects in each study phase. Incidence of OCT-detected dissection is presented for the total population and for each study phase. NIH = neointimal hyperplasia; OCT = optical coherence tomography; PCI = percutaneous coronary intervention; UH-CMC = University Hospitals Case Medical Center.

and stent area/lumen area ratio were calculated at the peristent region and the 5-mm edges to investigate the degree of vessel stretching by the stent.

Patient follow-up and clinical outcomes. Patients were followed up by telephone or hospital visit at 1, 6, and 12 months. MACE was recorded in a cumulative and hierarchical fashion, comprising the composite of death, nonfatal myocardial infarction (MI), and target lesion revascularization. Unless otherwise documented, all deaths were considered of cardiac origin. Occurrence of MI was defined according to the Joint ESC/ACCF/AHA/WHF Task Force for Redefinition of Myocardial Infarction (28). Target lesion revascularization was defined as any revascularization procedure (either PCI or coronary artery bypass graft) of the target lesion in the presence of angiographic restenosis and signs and symptoms of ischemia. Target vessel revascularization was defined as any repeat revascularization (either PCI or coronary artery bypass graft) of the target vessel, including upstream and downstream branches and the target lesion itself. Stent thromboses were classified according to the Academic Research Consortium criteria (29).

Statistical analysis. All statistical analyses were performed using SAS software version 9.2 (SAS Institute, Cary, North Carolina), and statistical significance was assessed at the 0.05 level. Continuous variables are expressed as mean ± SD, and categorical variables are expressed as counts and percentages. For per-patient analyses, differences between the 2 groups were evaluated by the unpaired Student *t* test for continuous variables, and Fisher exact test for categorical variables. To estimate the differences between the 2 groups at the lesion or segment level, multilevel mixed models (which can address random effects at lesion, vessel, and subject levels) were used for binary and continuous outcomes comparison. Multivariate logistic regression models considering hierarchical data structure were developed, and odds ratios (ORs) were used to evaluate factors associated with dissection identification after adjusting significant univariate predictors.

Results

Incidence of OCT-detected stent edge dissection. Overall, 321 patients (345 lesions in 339 vessels) underwent intracoronary OCT investigation between September 2010 and June 2011, and during this period, OCT was performed after stenting in 266 patients (290 lesions in 276 vessels). After excluding cases in which OCT analysis could not be performed in part or in all of the pre-defined 5-mm edge segments, there were available for the final analysis a total of 395 stent edges (from 249 lesions in 236 vessels of 230 patients). A flowchart with the reasons for exclusion and the number of cases included in each phase of the study is presented in Figure 3. Overall, the incidence of OCT-detected stent edge dissection was 39.1% per patient (90 of 230 patients), 38.6% per vessel (91 of 236 vessels), 37.8% per lesion (94 of 249 lesions), and 26.8% per stent edge (106 of 395 edges). Although not significant, OCT-detected edge dissections were slightly more frequent during the study's Phase II (42.6% [52 of 122] of the patients; 41.7% [53 of 127] of the vessels; 40.9% [56 of 137] of the lesions;

Table 1. Baseline Clinical Characteristics

	Overall (n = 230)	Dissection (n = 90)	No Dissection (n = 140)	p Value
Age, yrs	63.04 ± 12.27	66.97 ± 11.13	60.50 ± 12.34	<0.001
Male	148 (64.3)	54 (60.0)	94 (67.1)	0.270
Diabetes mellitus	71 (30.9)	33 (36.7)	38 (27.1)	0.127
Hypertension	187 (81.3)	79 (87.8)	108 (77.1)	0.044
Dyslipidemia	182 (79.1)	76 (84.4)	106 (75.7)	0.112
Smoking (current)	74 (32.2)	18 (20.0)	56 (40.0)	0.002
Prior MI	71 (30.9)	32 (35.6)	39 (27.9)	0.217
Prior PCI	63 (27.4)	26 (28.9)	37 (26.4)	0.683
Prior CABG	18 (7.8)	7 (7.8)	11 (7.9)	0.983
PCI indication				0.043
Silent ischemia	17 (7.4)	10 (11.1)	7 (5.0)	
Stable angina	55 (23.9)	20 (22.2)	35 (25)	
ACS				
Unstable angina	63 (27.4)	29 (32.2)	34 (24.3)	
NSTEMI	53 (23.0)	22 (24.4)	31 (22.1)	
STEMI	42 (18.3)	9 (10.0)	33 (23.6)	

Values are mean ± SD or n (%). p Value is for comparison between patients with and without stent edge dissection.

ACS = acute coronary syndrome; CABG = coronary artery bypass graft; MI = myocardial infarction; NSTEMI = non–ST-segment elevation myocardial infarction; PCI = percutaneous coronary intervention; STEMI = ST-segment elevation myocardial infarction.

and 28% [60 of 214] of the analyzed edges) than in Phase I (35.2% [38 of 108] of the patients; 34.9% [38 of 109] of the vessels; 33.9% [38 of 112] of the lesions; and 25.4% [46 of 181] of the edges; p = 0.280 for patient-level, p = 0.369 for vessel-level, p = 0.371 for lesion-level, and p = 0.542 for edge-level comparisons). Dissections were more frequently located at distal edges (67.9%; 72 of 106 edges) than at proximal edges (32.1%; 34 of 106 edges). Nine of 90 patients (10%) presented dissections at both distal and proximal edges of the same lesion, and 4 patients (4.4%) presented at least 1 dissection in more than 1 treated lesion in the same vessel.

Baseline clinical, angiographic, and procedural characteristics. Baseline clinical characteristics are presented in Table 1. The population with stent edge dissection was older, had higher rates of hypertension, and had a lower incidence of smokers in comparison to the group without dissection. Acute coronary syndromes were responsible for 68.7% of all PCI indications. Baseline angiographic characteristics are presented in Table 2. The left anterior descending artery was the most frequently treated vessel in both groups. In comparison to the group without dissection, patients with edge dissection had more complex (American College of Cardiology/American Heart Association type B2/C) lesions (79.8% vs.

Table 2. Baseline Angiographic Data

	Overall (n = 249 Lesions)	Dissection (n = 94 Lesions)	No Dissection (n = 155 Lesions)	p Value
Target vessel				0.168
LAD	114 (45.6)	41 (43.6)	73 (47.1)	
LCX	59 (23.6)	24 (25.5)	35 (22.6)	
RCA	67 (26.8)	25 (26.6)	42 (27.1)	
LM	3 (1.2)	3 (3.2)	0 (0.0)	
SVG	6 (2.4)	1 (1.1)	5 (3.2)	
Angulation >60°	22 (8.8)	14 (14.9)	8 (5.2)	0.041
Calcium (severe)	62 (24.9)	40 (42.5)	22 (14.2)	0.002
Bifurcation	46 (18.5)	9 (9.6)	37 (23.8)	0.031
Total occlusion (>3 months)	2 (0.8)	1 (1.1)	1 (0.6)	0.732
In-stent restenosis	17 (6.8)	7 (7.4)	10 (6.5)	0.806
ACC/AHA lesion class				0.034
A/B1	76 (30.5)	19 (20.2)	57 (36.8)	
B2/C	173 (69.5)	75 (79.8)	98 (63.2)	
Pre-PCI TIMI flow grade				0.521
0–2	45 (18.1)	15 (16.0)	30 (19.3)	
3	204 (81.9)	79 (84.0)	125 (80.7)	
Lesion length, mm	19.75 ± 12.52	22.01 ± 13.05	18.38 ± 12.02	0.091
Reference vessel diameter, mm	2.81 ± 0.74	2.61 ± 0.67	2.93 ± 0.76	0.011
Minimum lumen diameter, mm	0.80 ± 0.52	0.69 ± 0.47	0.88 ± 0.55	0.027
Diameter stenosis, %	70.85 ± 17.10	71.81 ± 19.56	69.81 ± 16.39	0.419
Stents per lesion	1.21 ± 0.47	1.30 ± 0.50	1.16 ± 0.41	0.020
Stent type				0.084
Xience V/Promus	185 (74.3)	79 (84.0)	106 (68.4)	
Cypher	95 (38.2)	32 (34.0)	63 (40.6)	
Endeavor	3 (1.2)	3 (3.2)	0 (0.0)	
BMS	19 (7.6)	8 (8.5)	11 (7.1)	
Nominal stent diameter, mm	2.99 ± 0.46	2.91 ± 0.39	3.03 ± 0.48	0.019
Total stented length, mm	26.63 ± 12.66	29.06 ± 13.99	25.19 ± 11.60	0.028
Maximum balloon diameter, mm	3.30 ± 0.57	3.16 ± 0.48	3.38 ± 0.59	0.002
Maximum inflation pressure, atm	18.02 ± 3.66	18.24 ± 3.88	17.89 ± 3.52	0.484
Post-PCI TIMI flow				0.734
0–2	2 (0.8)	1 (1.1)	1 (0.6)	
3	247 (99.2)	93 (98.9)	154 (99.4)	

Values are n (%) or mean ± SD. p value is for comparison between lesions with and without stent edge dissection.

ACC/AHA = American College of Cardiology/American Heart Association; BMS = bare metal stent(s); LAD = left anterior descending artery; LCX = left circumflex artery; LM = left main coronary artery; PCI = percutaneous coronary intervention; RCA = right coronary artery; SVG = saphenous vein graft; TIMI = Thrombolysis In Myocardial Infarction.

63.2%, p = 0.034), higher prevalence of severe vessel angulation (14.9% vs. 5.2%, p = 0.041), and severe calcification (42.6% vs. 14.3%, p = 0.002), smaller reference vessel diameters (2.61 ± 0.67 vs. 2.93 ± 0.76, p = 0.011), and smaller minimal lumen diameters (0.69 ± 0.47 vs. 0.88 ± 0.55, p = 0.027).

Only 17 (16%) of the total 106 edge dissections identified by OCT were also visualized by angiography, of which 14 (82.4%) were deemed type A, and 3 (17.6%) type B. Lesions with OCT-detected edge dissection had a higher prevalence of haziness (2.1% vs. 5.7%, p = 0.084) and step-up/step-down (8.8% vs. 19.8%, p = 0.001) by angiography. There were no cases of false-positive dissections indicated by angiography. No significant angiographic differences were observed between distal and proximal dissected edges (Fig. 4).

OCT qualitative assessment of stent edges. Qualitative assessment of stent edges by OCT is presented in Table 3. Overall, a high frequency of atherosclerotic plaques was seen at stent edges, particularly at OCT-detected dissected edges (95.3% vs. 75.4%, p < 0.001). Fibrotic plaques were more frequent in nondissected edges (50.0% vs. 35.6%, p = 0.029). Edges with dissection had wider (125.76 ± 77.94° vs. 65.39 ± 44.30°, p < 0.001) and more superficial calcifications (calcium-to-lumen distance: 0.07 ± 0.07 mm vs. 0.15 ± 0.12 mm, p = 0.002) than nondissected edges. Likewise, lipid plaques in dissected edges showed a trend towards a larger circumferential distribution, and had smaller minimum FC thickness (65.90 ± 38.33 μm vs. 103.07 ± 44.63 μm, p = 0.018). TCFAs were significantly more frequent at dissected edges than at nondissected edges (58.3% vs. 19%, p = 0.037).

Atherosclerotic disease was similarly encountered at both distal and proximal dissected edges. Although fibrotic plaques were more prevalent at distal edges (47.1% vs. 12.1%, p = 0.022), lipid plaques had significantly thinner FCs at proximal edges (60.83 ± 30.90 μm vs. 70.97 ± 45.41 μm, p = 0.044) (Online Table 1).

OCT quantitative assessment of stent edges. Quantitative OCT assessment is also presented in Table 3. Despite higher stent eccentricity in edges with dissection (0.11 ± 0.08 vs. 0.08 ± 0.05, p < 0.001), similar stent areas were observed in

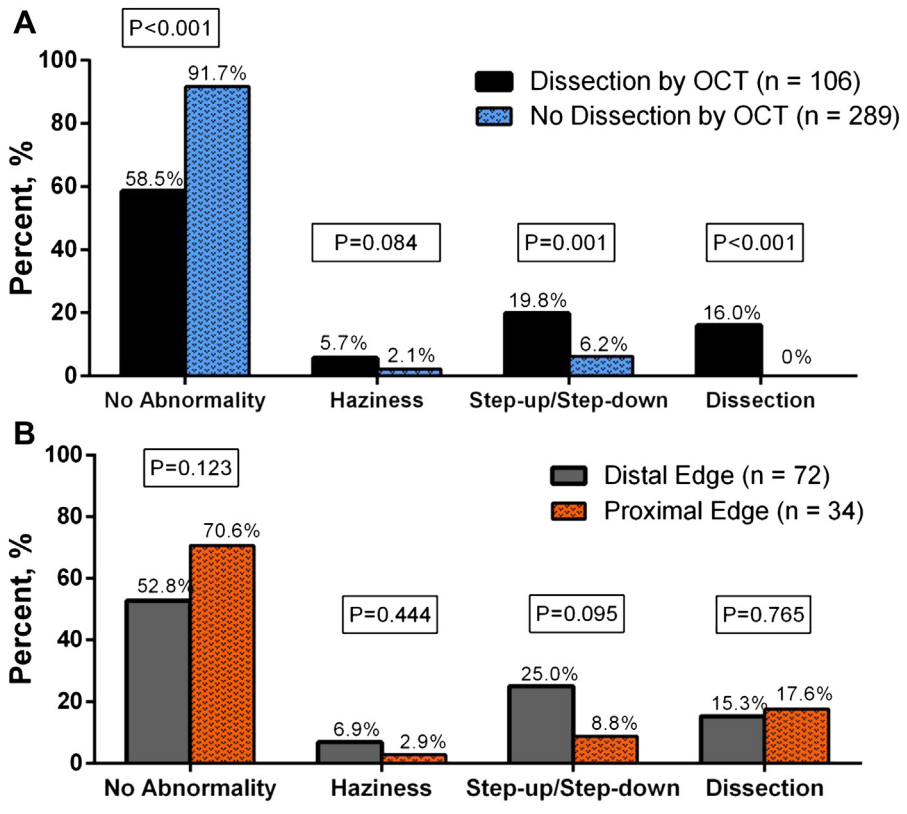

Figure 4. Angiographic Appearance of Stent Edges

(A) Angiographic appearance of edges with and without dissection. **(B)** Angiographic appearance of distal and proximal dissected edges as detected by optical coherence tomography (OCT).

Table 3. OCT Qualitative and Quantitative Analyses of Stent Edges

	Dissection (n = 106)	No Dissection (n = 289)	p Value
Plaque characteristics			
Stent landing region			
"Normal" vessel	5 (4.7)	71 (24.6)	<0.001
Presence of atherosclerotic plaque	101 (95.3)	218 (75.4)	<0.001
Circumferential distribution	36 (35.6)	79 (36.2)	0.238
Eccentric distribution	65 (64.4)	139 (63.8)	0.031
Plaque type			
Fibrotic	36/101 (35.6)	109/218 (50.0)	0.029
Fibrocalcific	41/101 (40.6)	67/218 (30.7)	0.137
Lipid-rich	24/101 (23.8)	42/218 (19.3)	0.351
Calcium quantification			
Angle, degrees	125.76 ± 77.94	65.39 ± 44.30	<0.001
Calcium-to-lumen distance, mm	0.07 ± 0.07	0.15 ± 0.12	0.002
Lipid-rich plaque quantification			
FC surface area, mm^2	0.44 ± 0.17	0.34 ± 0.16	0.070
Average FC thickness, μm	149.33 ± 43.40	167.40 ± 54.11	0.209
Minimal FC thickness, μm	65.90 ± 38.33	103.07 ± 44.63	0.018
TCFA	14/24 (58.3)	8 (19.0)	0.037
Quantitative measurements			
Stent border (inside the stent)			
Stent area, mm^2	6.51 ± 2.76	7.43 ± 2.97	0.208
Stent eccentricity index	0.11 ± 0.08	0.08 ± 0.05	<0.001
5-mm stent edge (outside the stent)			
Lumen area, mm^2	5.80 ± 3.34	8.00 ± 3.59	<0.001
MLA, mm^2	4.76 ± 3.15	7.08 ± 3.34	<0.001
Lumen eccentricity index	0.22 ± 0.07	0.14 ± 0.08	<0.001
Post-PCI diameter stenosis, %	20.02 ± 8.88	13.54 ± 7.27	<0.001
Post-PCI area stenosis, %	20.28 ± 11.70	11.96 ± 8.22	<0.001
Vascular stretching			
Peristent region			
SD/LD	0.1. ± 0.07	0.96 ± 0.06	<0.001
SA/LA	1.05 ± 0.26	0.91 ± 0.11	<0.001
5-mm stent edge			
SD/mean LD	1.10 ± 0.12	0.98 ± 0.10	<0.001
SA/mean LA	1.20 ± 0.26	0.96 ± 0.19	<0.001

Values are n (%) or mean ± SD.

FC = fibrous cap; LA = lumen area; LD = lumen diameter; MLA = minimum lumen area; OCT = optical coherence tomography; PCI = percutaneous coronary intervention; SA = stent area; SD = stent diameter; TCFA = thin-cap fibroatheroma.

both dissected and nondissected edges. Mean lumen area and minimal lumen area were significantly smaller in dissected edges, with higher lumen eccentricity in comparison to nondissected edges. After PCI, percent diameter stenosis and percent area stenosis were also significantly higher in dissected edges.

Dissected edges had significantly higher stent/artery ratios. Interestingly, in comparison to distal dissected edges, proximal dissected edges presented significantly smaller stent diameter/lumen diameter (1.04 ± 0.13 vs. 1.13 ± 0.11, p = 0.005) and stent area/lumen area (1.07 ± 0.24 vs. 1.27 ± 0.25, p = 0.006) ratios, suggesting that mechanisms beyond vessel overstretching may contribute to dissections at proximal stent edges (Online Table 1).

Predictors of OCT-detected stent edge dissection. Key independent predictors for OCT-detected edge dissections were the presence of atherosclerotic plaque at stent edges, angle of calcification in fibrocalcific plaques, minimum FC thickness in lipid-rich plaques, presence of TCFAs, stent and lumen eccentricity, stent-to-lumen diameter, and area ratios (Fig. 5).

Qualitative and morphometric analysis of stent edge dissections. Overall, longitudinal dissection length measured 2.04 ± 1.60 mm, and the majority of dissections appeared as flaps (96.2%). Forty-one dissected edges (38.7%) had more than 1 flap, and in 9 (8.5%) edges, flap and cavity coexisted. In most dissections, the depth of vascular injury was beyond the intimal/atheroma layer (48.1% medial and 4.7% adventitial). Intramural hematoma was detected in 10 (9.4%) dissected edges, with 9 of them located at distal edges. Only 1 intramural hematoma (10%) was located at a nondiseased edge, and 9 (90%) were located at sites with eccentric plaque. Intraluminal thrombus was detected in 4 (3.8%) dissected edges, with equal distribution between distal and proximal edges (Table 4). Dissections concomitantly identified by OCT and angiography (n = 17) were longer, had bigger flap dimensions, and had deeper vessel injury than dissections seen only by OCT (n = 89). All dissections seen by both OCT and angiography extended beyond the intimal/atheroma layer (Online Table 2).

Management of stent edge dissections. Of all 106 dissections, 24 (22.6%) were treated with additional stents. Treated dissections were longer and had more flaps per dissection, bigger flap dimensions, and deeper degrees of vascular injury in comparison to the dissections not treated (Table 5). Incidence of intramural hematoma was similar between the groups, and a trend was observed towards more intraluminal thrombus in treated dissections. Of all 24 dissections treated, 13 (54.2%) had been identified by both OCT and angiography, representing 76.5% of all 17 angiography-detected dissections. The rate of dissection treatment was not significantly different between the study's Phase I (9 of 46 [19.5%]) and Phase-II (15 of 60 [25%], p = 0.641), and no significant differences were observed regarding the morphometric parameters of dissections between the 2 study phases (Table 5). Factors identified by the multilevel univariate logistic regression analysis that predicted the decision to treat an OCT-detected dissection were the concomitant identification of dissection by angiography, dissection longitudinal length, and specific morphometric parameters by OCT (Table 6).

Clinical outcomes. Clinical follow-up was available for 211 (91.74%) of the total 230 patients included in the study (88 of 90 patients [97.7%] with OCT-detected edge dissections and 123 of 140 patients [87.8%] without dissections)

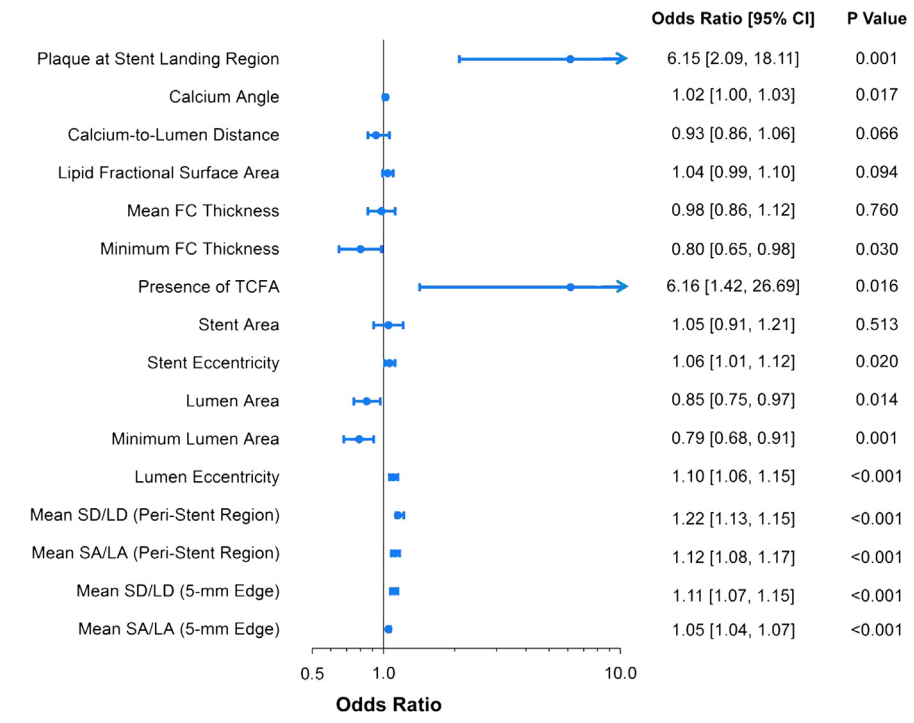

Figure 5. Multivariate Logistic Regression Analysis for Identification of Independent Predictors of OCT-Detected Stent Edge Dissections

Forest plot and odds ratios show the association of several factors and the occurrence of stent edge dissection after adjusting significant univariate clinical, angiographic, and procedural predictors. CI = confidence interval; LA = lumen area; LD = lumen diameter; SA = stent area; SD = stent diameter; TCFA = thin-cap fibroatheroma; other abbreviations as in Figure 1.

(Table 7). The mean follow-up time was 11.49 ± 1.63 months for patients with dissection and 11.02 ± 2.48 months for patients without dissection (p = 0.120). There were a total of 14 MACE (7 of 88 [7.95%] patients with dissection vs. 7 of 123 [5.69%] patients without dissection [p = 0.581]). In the dissection group, there were 3 deaths (1 of cardiac origin) and 4 nonfatal MIs, from which only 1 was related to the target lesion requiring revascularization. Of note, all events occurred more than 30 days after the index procedure, and happened in patients in whom the dissections were only seen by OCT, as the majority of dissections concomitantly seen by OCT and angiography were treated. Edge dissections in patients with and without MACE had similar morphometric characteristics (Online Tables 3 and 4).

In the group of patients without dissection, there were 5 deaths (4 of cardiac origin) and 2 nonfatal MIs, from which 1 was due to severe in-stent restenosis and required revascularization. There were no stent thrombosis in the edge dissection group and only 1 probable stent thrombosis in a patient without dissection who had a cardiac death in the first week after the index procedure (Table 7).

Discussion

We report the first large comprehensive OCT evaluation of arterial wall injury at stent edges in the daily clinical practice. The present study led to the following observations: 1) edge dissections after stenting are frequently detected by OCT, with a "true" incidence of 33.9% when OCT was performed in all treated vessels (Phase I) or a "real-world" rate of 40.9% when OCT was selectively used per the operator's discretion (Phase II); 2) most OCT-detected edge dissections (84%) were not apparent on angiography; 3) atherosclerotic disease was frequent (95.3%) at dissected edges, with the odds of having a dissection increasing by more than 6 times in the presence of a plaque; 4) circumferential calcium angle, FC thickness over lipid-rich plaques, and vessel overstretching by the stent were independent predictors for the occurrence of edge dissections; 5) a relatively high frequency (22.6%) of OCT-detected dissections were treated with additional stenting, which was driven by the concomitant presence of dissection on angiography in addition to OCT findings; and 6) patients with untreated OCT-detected edge dissections had similar 12-month outcomes compared with patients without dissection.

Table 4. OCT Qualitative and Morphometric Analysis of Dissected Edges

	Overall (n = 106)	Distal Edge (n = 72)	Proximal Edge (n = 34)	p Value
Dissection longitudinal length, mm	2.04 ± 1.60	2.03 ± 1.60	2.06 ± 1.65	0.951
Dissection appearance on OCT				
Flap	102 (96.2)	69 (95.8)	33 (97.1)	0.768
Cavity	13 (12.3)	9 (12.5)	4 (11.8)	0.917
Number of flaps per dissection	1.45 ± 0.77	1.40 ± 0.69	1.56 ± 0.93	0.372
Number of cavities per dissection	0.12 ± 0.33	0.13 ± 0.33	0.12 ± 0.33	0.895
Maximum flap depth, mm	0.62 ± 0.39	0.60 ± 0.40	0.65 ± 0.39	0.553
Maximum flap opening, mm	0.39 ± 0.34	0.37 ± 0.36	0.42 ± 0.28	0.489
Maximum flap length, mm	1.09 ± 0.67	1.05 ± 0.70	1.19 ± 0.61	0.324
Maximum flap area, mm^2	0.39 ± 0.39	0.37 ± 0.39	0.45 ± 0.37	0.337
Maximum cavity depth, mm	0.46 ± 0.25	0.43 ± 0.29	0.52 ± 0.16	0.581
Maximum cavity opening, mm	0.64 ± 0.26	0.62 ± 0.30	0.68 ± 0.19	0.751
Maximum cavity area, mm^2	0.20 ± 0.16	0.17 ± 0.18	0.26 ± 0.11	0.380
Intramural hematoma	10 (9.4)	9 (12.5)	1 (2.9)	0.194
Hematoma longitudinal length	1.91 ± 1.84	2.03 ± 1.91	0.80	N/A
Maximum hematoma Area, mm^2	0.92 ± 0.60	0.88 ± 0.63	1.19	N/A
Intraluminal thrombus	4 (3.8)	2 (2.8)	2 (5.9)	0.464
Depth of vessel injury				
Intimal	50 (47.2)	34 (47.2)	16 (47.1)	0.984
Medial	51 (48.1)	34 (47.2)	17 (50.0)	0.803
Adventitial	5 (4.7)	4 (5.6)	1 (2.9)	0.574

Values are mean ± SD or n (%). p value is for comparison between OCT-detected dissection at the distal and proximal edges.
OCT = optical coherence tomography.

Incidence of stent edge dissection. Edge dissections post-stenting have been observed in 5% to 23% of cases examined by IVUS (3,30). A recent OCT investigation reported the presence of stent edge dissections in 25% of 73 patients (14). During the first phase of the present study, edge dissections were detected in 33.9% of 116 treated lesions examined by OCT. Although these figures may represent the "true" incidence of OCT-detected stent edge dissection, the expected incidence of dissections in everyday practice may be relatively higher (40.9%), likely because of more selective use of OCT. Our findings further confirm that dissections are twice more likely to occur in distal edges in comparison to proximal edges (67.9% vs. 32.1%) (7,14).

Predictors for stent edge dissection. Incomplete lesion coverage has been associated with increased risk of procedural complications and poor clinical outcomes (31,32). The somewhat expected, yet alarming, high prevalence of "untreated disease" found at stent margins is in part related to PCI technique and limitations of angiography to properly determine disease severity and extension. Only 4.7% of all dissected edges were free of disease by OCT, contrasting to 24.6% of the nondissected edges ($p < 0.001$). The odds of having an edge dissection were 6 times higher when the stent was placed over a diseased region than over a normal vessel (OR: 6.15, 95% confidence interval: 2.09 to 18.11, $p = 0.001$). These results are in line with previous IVUS observations (30,33) and underscores a modifiable factor, that is, judicious PCI technique to minimize longitudinal geographic miss, that may further improve PCI results.

Beyond the presence of disease at stent edges, the type of plaque may also play an important role in the pathogenesis of edge dissections. Previous work utilizing IVUS to understand angiographic haziness at stent edges demonstrated a significantly higher prevalence of echolucent "soft" plaques in patients with peristent injury than in controls (20). In the current study, the majority of plaques were fibrotic or fibrocalcific in both dissected and nondissected edges, and OCT-defined lipid-rich plaques represented only 23.8% of plaques at dissected edges. Differences between OCT and IVUS properties to detect lipid may explain these somewhat discordant results on the association of lipid-rich plaques and stent dissection. Our study, however, expands upon these prior observations and shows that morphometric aspects of FC overlying lipid/necrotic core pose significant risk for edge dissections. The incidence of TCFA was higher in dissected edges than in nondissected edges, and minimum FC thickness over lipid-rich plaques was significantly smaller. Furthermore, FC thickness was identified as an independent predictor for the occurrence of edge dissections. Based on an exploratory receiver-operating characteristic curve analysis, a minimum FC thickness $\leq$80 μm was the best cutoff to predict stent edge dissection on a lipid-rich

Table 5. OCT Qualitative and Morphometric Analysis of Dissected Edges According to Study Phase and Management Strategy

	Study Phase			Management Strategy		
	Phase I (n = 46)	Phase II (n = 60)	p Value	Treated (n = 24)	Not Treated (n = 82)	p Value
Dissection longitudinal length, mm	2.04 ± 1.45	2.04 ± 1.73	0.991	3.03 ± 1.41	1.75 ± 1.55	0.007
Dissection appearance on OCT						
Flap	45 (97.8)	57 (95.0)	0.538	24 (100)	78 (95.1)	0.737
Cavity	5 (10.9)	8 (13.3)	0.740	1 (4.2)	12 (14.6)	0.246
Number of flaps per dissection	1.52 ± 0.81	1.40 ± 0.74	0.741	1.83 ± 0.76	1.34 ± 0.74	0.029
Number of cavities per dissection	0.11 ± 0.31	0.13 ± 0.34	0.545	0.04 ± 0.20	0.15 ± 0.36	0.219
Maximum flap depth, mm	0.64 ± 0.42	0.60 ± 0.38	0.674	0.93 ± 0.43	0.52 ± 0.33	0.003
Maximum flap opening, mm	0.36 ± 0.25	0.41 ± 0.39	0.570	0.58 ± 0.29	0.33 ± 0.33	0.014
Maximum flap length, mm	1.12 ± 0.64	1.07 ± 0.70	0.972	1.64 ± 0.58	0.93 ± 0.61	0.003
Maximum flap area, mm^2	0.44 ± 0.43	0.36 ± 0.35	0.402	0.73 ± 0.45	0.29 ± 0.30	0.002
Maximum cavity depth, mm	0.42 ± 0.21	0.49 ± 0.29	0.682	0.75	0.44 ± 0.25	N/A
Maximum cavity opening, mm	0.67 ± 0.25	0.62 ± 0.28	0.764	0.87	0.62 ± 0.26	N/A
Maximum cavity area, mm^2	0.20 ± 0.14	0.20 ± 0.18	0.990	0.41	0.18 ± 0.15	N/A
Intramural hematoma	5 (10.9)	5 (8.3)	0.790	3 (12.5)	7 (8.5)	0.680
Hematoma longitudinal length	1.96 ± 1.47	1.86 ± 2.34	0.938	1.73 ± 1.76	1.99 ± 2.01	0.882
Maximum hematoma area, mm^2	0.78 ± 0.52	1.05 ± 0.70	0.524	1.21 ± 0.69	0.79 ± 0.56	0.497
Intraluminal thrombus	2 (4.3)	2 (3.3)	0.812	3 (12.5)	1 (1.2)	0.083
Depth of vessel injury						
Intimal	19 (41.3)	31 (51.7)	0.403	3 (12.5)	47 (57.3)	0.014
Medial	26 (56.5)	25 (41.7)	0.270	17 (70.8)	34 (41.5)	0.049
Adventitial	1 (2.2)	4 (6.7)	0.410	4 (16.7)	1 (1.2)	0.051

Values are mean ± SD or n (%).
OCT = optical coherence tomography.

plaque, with a sensitivity and specificity of 73.9% and 72.5%, respectively.

Presence of calcification has been traditionally identified as an independent predictor of coronary dissection after either balloon angioplasty or stent implantation (7,34,35). Gonzalo et al. (14) assessed 24 stent edge dissections with OCT and found fibrocalcific plaques (43.8%) to be more frequent at distal dissected edges than were fibrotic plaques (10%, p = 0.009). In the current study, we found a similar frequency of fibrocalcific plaques in dissected edges (40.6%), but that was not significantly different from nondissected edges (30.7%, p = 0.137). Notwithstanding, the circumferential extension, but not the simple presence of calcification, was identified as an independent predictor of stent edge dissection (OR: 1.02 for every 1° increase; 95% CI: 1.00 to 1.03, p = 0.017). OCT enabled assessment of calcium depth, but this was not associated with occurrence

Table 6. Factors Influencing Decision to Treat an OCT-Detected Edge Dissection Based on Multilevel Univariate Logistic Regression Analysis

	Odds Ratio	95% Confidence Interval	p Value
Dissection identified by angiography	22.85	4.67–111.75	0.002
Maximum flap area, mm^2	21.73	3.10–152.51	0.008
Maximum flap depth, mm	14.67	2.40–89.79	0.011
Maximum flap opening	10.48	1.11–98.86	0.043
Maximum flap length	5.42	1.86–15.82	0.008
Number of flaps per dissection	2.20	1.05–4.62	0.039
Dissection length, mm	1.03	1.03–1.06	0.008

OCT = optical coherence tomography.

Table 7. Cumulative 12-Month Clinical Outcomes

	Dissection			
	Overall (n = 88)	Treated (n = 22)	Not Treated (n = 66)	No Dissection (n = 123)
MACE	7 (7.95%)	1 (4.54%)	6 (9.09%)	7 (5.69%)
All-cause death	3 (3.40%)	0	3 (4.54%)	5 (4.06%)
Cardiac death	1 (1.13%)	0	1 (1.51%)	4 (3.25%)
Nonfatal MI	4 (4.54%)	1 (4.54%)	3 (4.54%)	3 (2.43%)
TVR	1 (1.13%)	0	1 (1.51%)	1 (0.81%)
TLR	1 (1.13%)	0	1 (1.51%)	1 (0.81%)
Definite/probable stent thrombosis	0	0	0	1 (0.81%)

Values are n (%). There were no significant statistical differences between groups.
MACE = major adverse cardiac event(s); MI = myocardial infarction; TLR = target lesion revascularization; TVR = target vessel revascularization.

of dissection. An exploratory receiver-operating characteristic curve analysis revealed an angle of calcification ≥72° to be the best cutoff to predict calcium-related edge dissections, with a sensitivity of 71.1% and specificity of 71.2%. These results suggest that loss of circumferential vessel compliance might be more important in the pathogenesis of calcium-related dissections rather than the presence or depth of calcification.

Mechanical factors, such as vessel overstretching by an oversized stent relative to the reference vascular dimensions, have also been suggested as an important cause of dissection at stent edges. In the present study, we found significantly greater stent/artery ratios in dissected edges than in non-dissected edges. For every 1% increase in stent diameter/lumen diameter or stent area/lumen area ratios, the odds of having a dissection increased 22% and 12%, respectively. As anticipated, vessel overstretching was more pronounced in the distal compared with the proximal dissected edges. Of note, the mean stent/lumen diameter and area ratios of 1.04 and 1.07 indicate an adequate stent sizing at proximal edges, suggesting that other factors such as plaque type, FC thickness, and circumferential calcification play a more significant role in proximal edge dissections.

OCT assessment of stent edge dissections and management. Of all 106 dissections, 24 (22.6%) were treated with additional stents. As expected, treated dissections were longer, more complex, and deeper in comparison to the dissections left untreated. The presence of intramural hematoma did not impact the decision to treat; only 3 of the 10 dissections with intramural hematoma were treated. Operators were more prone to treat dissections observed on both OCT and angiography. Importantly, the time period of the study was not identified as a predictor for the decision to treat, indicating that the learning curve of interpreting OCT images did not influence the decision to further intervene upon dissected stent edges.

Clinical implications. The arterial wall usually responds to mechanical injury through a series of cellular and molecular mechanisms implicated in neointimal hyperplasia formation and vessel remodeling, which ultimately may lead to restenosis (36). In addition, plaque disruption with exposure of its prothrombotic milieu may promote acute/subacute thrombosis (6,7). In fact, stent edge dissections have been associated with increased short- and mid-term incidence of MACE and stent thrombosis (4–7,37). In the present study, the 12-month MACE rate was relatively low in patients with and without edge dissections detected by OCT. Furthermore, OCT morphometric characteristics of untreated dissections in patients who developed MACE were not significantly different than dissections in patients who had uneventful outcomes. Virtually all dissections presented with TIMI flow grade 3 at the end of the procedure and were classified as National Heart, Lung, and Blood Institute type B or less. These observations suggest that angiographically "silent" dissections seen only by OCT have minimal impact on outcomes after stent deployment in modern PCI. However, these findings should be interpreted with caution. The more severe OCT-detected dissections were treated. As a result, edge dissections left untreated were smaller in size, had shorter longitudinal extension, and were usually more superficial, with their depths limited to the intimal/atheroma layer (Table 6). Nevertheless, the present results are reassuring in that minor, non–flow-limiting OCT-detected dissections have a benign course and are not associated with an increased incidence of adverse outcomes (34,38–41).

Study limitations. The present study is insufficient to support specific criteria to guide clinical decision making on which OCT-detected dissection should be treated, but it indicates that dissections with longitudinal length ≤1.75 mm, with <2 concomitant flaps, flap depth ≤0.52 mm, flap opening ≤0.33 mm, and not extending deeper than the media layer have favorable outcomes and can be left untreated. Future studies would be required to understand whether the more complex characteristics of the treated dissections in the present study would be associated with poor outcomes if left untreated. However, such study will be difficult to be conducted due to the inherently ethical limitations of leaving potentially life-threatening vascular complications untreated. Another potential limitation is that the absence of serial OCT examination precludes conclusions on the mechanisms of stent edge dissection healing and determination of predictors for dissection persistence over time, aspects that need to be investigated in future works.

Conclusions

Utilization of OCT in daily practice reveals a high rate of stent-edge dissections. Dissections were associated with atherosclerosis at the stent edge and PCI technique. A small minority of dissections was angiographically evident, though with detailed OCT assessment, subsequent management was altered. Non–flow-limiting, short, and superficial dissections proved to be benign when left untreated.

Reprint requests and correspondence: Dr. Marco A. Costa, Division of Cardiology, Harrington Heart & Vascular Institute, University Hospitals Case Medical Center, Case Western Reserve School of Medicine, 11,100 Euclid Avenue, Lakeside 3001, Cleveland, Ohio 44106. E-mail: marco.costa@uhhospitals.org.

REFERENCES

1. Waller BF. "Crackers, breakers, stretchers, drillers, scrapers, shavers, burners, welders and melters"—the future treatment of atherosclerotic coronary artery disease? A clinical-morphologic assessment. J Am Coll Cardiol 1989;13:969–87.
2. Farb A, Virmani R, Atkinson JB, Kolodgie FD. Plaque morphology and pathologic changes in arteries from patients dying after coronary balloon angioplasty. J Am Coll Cardiol 1990;16:1421–9.

3. Sheris SJ, Canos MR, Weissman NJ. Natural history of intravascular ultrasound-detected edge dissections from coronary stent deployment. Am Heart J 2000;139:59–63.
4. Cutlip DE, Baim DS, Ho KK, et al. Stent thrombosis in the modern era: a pooled analysis of multicenter coronary stent clinical trials. Circulation 2001;103:1967–71.
5. Cheneau E, Leborgne L, Mintz GS, et al. Predictors of subacute stent thrombosis: results of a systematic intravascular ultrasound study. Circulation 2003;108:43–7.
6. Rogers JH, Lasala JM. Coronary artery dissection and perforation complicating percutaneous coronary intervention. J Invasive Cardiol 2004;16:493–9.
7. Biondi-Zoccai GG, Agostoni P, Sangiorgi GM, et al. Incidence, predictors, and outcomes of coronary dissections left untreated after drug-eluting stent implantation. Eur Heart J 2006;27:540–6.
8. Choi SY, Witzenbichler B, Maehara A, et al. Intravascular ultrasound findings of early stent thrombosis after primary percutaneous intervention in acute myocardial infarction: a Harmonizing Outcomes with Revascularization and Stents in Acute Myocardial Infarction (HORIZONS-AMI) substudy. Circ Cardiovasc Interv 2011;4:239–47.
9. Holmes DR Jr., Holubkov R, Vlietstra RE, et al. Comparison of complications during percutaneous transluminal coronary angioplasty from 1977 to 1981 and from 1985 to 1986: the National Heart, Lung, and Blood Institute Percutaneous Transluminal Coronary Angioplasty Registry. J Am Coll Cardiol 1988;12:1149–55.
10. Baptista J, di Mario C, Ozaki Y, et al. Impact of plaque morphology and composition on the mechanisms of lumen enlargement using intracoronary ultrasound and quantitative angiography after balloon angioplasty. Am J Cardiol 1996;77:115–21.
11. Bezerra HG, Costa MA, Guagliumi G, Rollins AM, Simon DI. Intracoronary optical coherence tomography: a comprehensive review clinical and research applications. J Am Coll Cardiol Intv 2009;2:1035–46.
12. Bouma BE, Tearney GJ, Yabushita H, et al. Evaluation of intracoronary stenting by intravascular optical coherence tomography. Heart 2003;89:317–20.
13. Gonzalo N, Serruys PW, Okamura T, et al. Optical coherence tomography assessment of the acute effects of stent implantation on the vessel wall: a systematic quantitative approach. Heart 2009;95:1913–9.
14. Gonzalo N, Serruys PW, Okamura T, et al. Relation between plaque type and dissections at the edges after stent implantation: an optical coherence tomography study. Int J Cardiol 2011;150:151–5.
15. Kume T, Okura H, Miyamoto Y, et al. Natural history of stent edge dissection, tissue protrusion and incomplete stent apposition detectable only on optical coherence tomography after stent implantation - preliminary observation. Circ J 2012;76:698–703.
16. Stefano GT, Bezerra HG, Mehanna E, et al. Unrestricted utilization of frequency domain optical coherence tomography in coronary interventions. Int J Cardiovasc Imaging 2013;29:741–52.
17. Ellis SG, Vandormael MG, Cowley MJ, et al. Coronary morphologic and clinical determinants of procedural outcome with angioplasty for multivessel coronary disease. Implications for patient selection. Multivessel Angioplasty Prognosis Study Group. Circulation 1990;82:1193–202.
18. Mintz GS, Popma JJ, Pichard AD, et al. Patterns of calcification in coronary artery disease. A statistical analysis of intravascular ultrasound and coronary angiography in 1155 lesions. Circulation 1995;91:1959–65.
19. Gibson CM, de Lemos JA, Murphy SA, et al. Combination therapy with abciximab reduces angiographically evident thrombus in acute myocardial infarction: a TIMI 14 substudy. Circulation 2001;103:2550–4.
20. Ziada KM, Tuzcu EM, De Franco AC, et al. Intravascular ultrasound assessment of the prevalence and causes of angiographic "haziness" following high-pressure coronary stenting. Am J Cardiol 1997;80:116–21.
21. Haldis TA, Fenster B, Gavlick K, Singh KD, Iliadis E, Blankenship JC. The angiographic step-up and step-down: a surrogate for optimal stent expansion by intravascular ultrasound. J Invasive Cardiol 2007;19:101–5.
22. TIMI Study Group. The Thrombolysis in Myocardial Infarction (TIMI) trial. Phase I findings. N Engl J Med 1985;312:932–6.
23. Tearney GJ, Regar E, Akasaka T, et al. Consensus standards for acquisition, measurement, and reporting of intravascular optical coherence tomography studies: a report from the International Working Group for Intravascular Optical Coherence Tomography Standardization and Validation. J Am Coll Cardiol 2012;59:1058–72.
24. Velican D, Velican C. Comparative study on age-related changes and atherosclerotic involvement of the coronary arteries of male and female subjects up to 40 years of age. Atherosclerosis 1981;38:39–50.
25. Yabushita H, Bouma BE, Houser SL, et al. Characterization of human atherosclerosis by optical coherence tomography. Circulation 2002;106:1640–5.
26. Wang Z, Chamie D, Bezerra HG, et al. Volumetric quantification of fibrous caps using intravascular optical coherence tomography. Biomed Opt Express 2012;3:1413–26.
27. Burke AP, Farb A, Malcom GT, Liang YH, Smialek J, Virmani R. Coronary risk factors and plaque morphology in men with coronary disease who died suddenly. N Engl J Med 1997;336:1276–82.
28. Thygesen K, Alpert JS, White HD, et al., Joint ESC/ACCF/AHA/WHF Task Force for the Redefinition of Myocardial Infarction. Universal definition of myocardial infarction. J Am Coll Cardiol 2007;50:2173–95.
29. Cutlip DE, Windecker S, Mehran R, et al., Academic Research Consortium. Clinical end points in coronary stent trials: a case for standardized definitions. Circulation 2007;115:2344–51.
30. Liu X, Tsujita K, Maehara A, et al. Intravascular ultrasound assessment of the incidence and predictors of edge dissections after drug-eluting stent implantation. J Am Coll Cardiol Intv 2009;2:997–1004.
31. Lemos PA, Saia F, Ligthart JM, et al. Coronary restenosis after sirolimus-eluting stent implantation: morphological description and mechanistic analysis from a consecutive series of cases. Circulation 2003;108:257–60.
32. Costa MA, Angiolillo DJ, Tannenbaum M, et al. Impact of stent deployment procedural factors on long-term effectiveness and safety of sirolimus-eluting stents (final results of the multicenter prospective STLLR trial). Am J Cardiol 2008;101:1704–11.
33. Schwarzacher SP, Metz JA, Yock PG, Fitzgerald PJ. Vessel tearing at the edge of intracoronary stents detected with intravascular ultrasound imaging. Cathet Cardiovasc Diagn 1997;40:152–5.
34. Sharma SK, Israel DH, Kamean JL, Bodian CA, Ambrose JA. Clinical, angiographic, and procedural determinants of major and minor coronary dissection during angioplasty. Am Heart J 1993;126:39–47.
35. Fitzgerald PJ, Ports TA, Yock PG. Contribution of localized calcium deposits to dissection after angioplasty. An observational study using intravascular ultrasound. Circulation 1992;86:64–70.
36. Costa MA, Simon DI. Molecular basis of restenosis and drug-eluting stents. Circulation 2005;111:2257–73.
37. van Werkum JW, Heestermans AA, Zomer AC, et al. Predictors of coronary stent thrombosis: the Dutch Stent Thrombosis Registry. J Am Coll Cardiol 2009;53:1399–409.
38. Leimgruber PP, Roubin GS, Anderson HV, et al. Influence of intimal dissection on restenosis after successful coronary angioplasty. Circulation 1985;72:530–5.
39. Huber MS, Mooney JF, Madison J, Mooney MR. Use of a morphologic classification to predict clinical outcome after dissection from coronary angioplasty. Am J Cardiol 1991;68:467–71.
40. Bourassa MG, Lesperance J, Eastwood C, et al. Clinical, physiologic, anatomic and procedural factors predictive of restenosis after percutaneous transluminal coronary angioplasty. J Am Coll Cardiol 1991;18:368–76.
41. Hermans WR, Rensing BJ, Foley DP, et al. Therapeutic dissection after successful coronary balloon angioplasty: no influence on restenosis or on clinical outcome in 693 patients. The MERCATOR Study Group (Multicenter European Research Trial with Cilazapril after Angioplasty to prevent Transluminal Coronary Obstruction and Restenosis). J Am Coll Cardiol 1992;20:767–80.

Key Words: coronary dissection ■ optical coherence tomography ■ percutaneous coronary intervention ■ stent.

APPENDIX

For supplementary tables, please see the online version of this paper.